Experimental Animals
Exp. Anim. 73(1), 50–60, 2024

Original

Nucleic acid sensing Toll-like receptors 3 and 9 play complementary roles in the development of bacteremia after nasal colonization associated with influenza co-infection

Denisa NANUSHAJ*, Masamitsu KONO*, Hideki SAKATANI, Daichi MURAKAMI and Muneki HOTOMI

Department of Otorhinolaryngology-Head and Neck Surgery, Wakayama Medical University, Research Building 9F, 811-1 Kimiidera, Wakayama 641-8510, Japan

Abstract: *Streptococcus pneumoniae* can cause mortality in infant, elderly, and immunocompromised individuals owing to invasion of bacteria to the lungs, the brain, and the blood. In building strategies against invasive infections, it is important to achieve greater understanding of how the pneumococci are able to survive in the host. Toll-like receptors (TLRs), critically important components in the innate immune system, have roles in various stages of the development of infectious diseases. Endosomal TLRs recognize nucleic acids of the pathogen, but the impact on the pneumococcal diseases of immune responses from signaling them remains unclear. To investigate their role in nasal colonization and invasive disease with/without influenza co-infection, we established a mouse model of invasive pneumococcal diseases directly developing from nasal colonization. TLR9 KO mice had bacteremia more frequently than wildtype in the pneumococcal mono-infection model, while the occurrence of bacteremia was higher among TLR3 KO mice after infection with influenza in advance of pneumococcal inoculation. All TLR KO strains showed poorer survival than wildtype after the mice had bacteremia. The specific and protective role of TLR3 and TLR9 was shown in developing bacteremia with/without influenza co-infection respectively, and all nucleic sensing TLRs would contribute equally to protecting sepsis after bacteremia.
Key words: bacteremia, invasive pneumococcal disease, nasal colonization, *Streptococcus pneumoniae*, Toll-like receptors

Introduction

Recent development of various molecular biological techniques has enabled to elucidate detailed mechanisms for many diseases, however, establishing animal models is still a critical way to better reflect disease progression, such as infectious diseases that always require to evaluate host-pathogen's interactions [1, 2]. *Streptococcus pneumoniae* is a Gram-positive bacterium which is a particular challenge for neonates and the elderly adults. Previous studies have concentrated on the phenomena associated with colonization, carriage rate and transmission [3–9]. However, the events occurring after *S. pneumoniae* breaks the first barriers of protection in the nasopharynx, the invasion of the host, are still not understood. Invasion is the main cause of the morbidity of *S. pneumoniae* because the bacteria can migrate to sterile sites such as the blood or the central nervous system [10]. The innate immune receptors are mostly associated with the responses of the host to pathogens,

(Received 1 January 2023 / Accepted 30 July 2023 / Published online in J-STAGE 3 August 2023)
Corresponding authors: M. Kono. email: ma332jp@wakayama-med.ac.jp
M. Hotomi. email: mhotomi@wakayama-med.ac.jp
**These authors contributed equally to this study.*
Supplementary Figures: refer to J-STAGE: https://www.jstage.jst.go.jp/browse/expanim

such as Toll-like Receptor (TLR) families [11]. The cell surface TLRs recognize sugar chains or proteins derived from pathogens. For recognition of the pneumococcus, TLR2 and TLR4 have been known to be activated by lipoteichoic acid and pneumolysin, respectively [12–15]. On the other hand, other types of TLRs are located in the endosome and recognize nucleic acid derived from pathogens. TLR3 is highly activated by viral double stranded RNA resulting in production of type I interferon and anti-viral host responses [16, 17]. Mouse TLR7 and human TLR8 are phylogenetically and structurally related and they recognize the single stranded viral RNA, although they are expressed in different cells [18]. TLR9 recognizes and activates DNA with CpG motifs derived from bacteria or viruses, and induces various innate immune responses [19]. The impacts of these nucleic acid sensing receptors on the pneumococcal infections have been described, but with disparity in the conclusions [20–24]. In this study, we used a mouse model to evaluate the roles of nucleic acid sensing TLRs in the development of pneumococcal invasive infections arising from nasal carriage.

Material and Methods

Animals

C57BL/6J mice were obtained from Charles River Laboratories (Yokohama, Japan). Mice of C57BL/6J background, knockouts for TLR3, TLR7, or TLR9 activity were donated by Prof. Tsuneyasu Kaisho (the Department of Immunology, Institute of Advanced Medicine Wakayama Medical University) and Prof. Shizuo Akira (the Laboratory of Host Defense, WPI Immunology Frontier Research Center (IFReC), Osaka University) [18, 25, 26]. Unc93b1 KO mice were kindly provided by Prof. Kensuke Miyake (the Institute of Medical Science, University of Tokyo) [27]. Unc93b1 is one of the key carrier proteins to transport TLR3, TLR7 and TLR9 to an endosome, which is required to activate these receptors. All mice used in this study were maintained under a specific pathogen-free condition from the onset in individually ventilated cages.

Pneumococcal and influenza strains and growth conditions

P2431, a serotype 6A of *S. pneumoniae*, was used throughout the present study [28]. This strain is streptomycin-resistant, and it has good ability in colonization establishment and lethal bacteremia development. Another strain used was TIGR4, a serotype 4, which was previously used in a different experiment to check the nasal colonization in the mice [9]. Bacteria were grown up to the mid-log phase in Tryptic Soy Broth (Becton Dickinson (BD) Franklin Lakes, NJ, USA), mixed with 20% glycerol and stored at −80°C. The mouse-adapted strain of influenza virus A/HKx31 (H3N2) was a kind gift from Prof. Jeffry N. Weiser (New York University). Viral concentrations were determined and adjusted by titration in Madin-Darby Canine Kidney cells, as described previously [29].

Murine infection model

The experimental scheme is shown in Fig. 1. Six-week-old mice were inoculated intranasally (i.n.) with 10 μl of the pneumococcal suspension to each nostril (5×10^7 CFU/mouse) without anesthesia. The influenza co-infection mice were initially treated with 2×10^2–2×10^4 $TCID_{50}$ of influenza A and then pneumococci two days later [30]. After each experiment, quantitative culture was performed to determine the actual number of inoculated bacteria. Mice were euthanized 48 h after the infection by isoflurane inhalation. The nasal cavity was lavaged with 200 μl of sterile PBS from a needle (26 gauge) inserted into the trachea, and the fluid was collected in tubes. For detection of bacteria in the lung, the lung was homogenized with 1 ml of sterile PBS. A cardiac puncture was performed to evaluate the bacteremia/sepsis, and the blood samples were serially diluted before coagulation. The other model of the co-infection consisted of infecting the mice with 10 μl of the pneumococ-

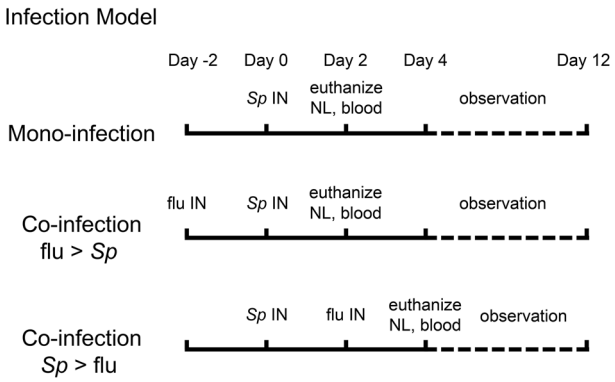

Fig. 1. Experimental schematics of this study. For the mono-infection group, mice were inoculated intranasally (IN) with *S. pneumoniae* (*Sp*) serotype 6A or TIGR4 on day 0. On day 2, mice were euthanized and the evaluation of the colony counts and flow cytometry was performed. For the co-infection group (influenza first, then *Sp*), mice were inoculated intranasally with influenza on day −2, and *Sp* serotype 6A or TIGR4 on day 0. On day 2, the mice were euthanized. For the co-infection group (*Sp* first, then influenza), mice were inoculated intranasally with *Sp* serotype 6A on day 0, and then influenza on day 2. On day 4, the mice were euthanized. For the survival experiment, the mice in each infection model were monitored every 12 h until day 12 after the pneumococcal infection.

cal suspension to each nostril (5×10^7 CFU/mouse) without anesthesia on day 0 and then influenza two days after that. All samples were serially diluted on a 96-well plate by mixing thoroughly and were plated on a blood plate for quantitative evaluation. The limit of detection was 666 CFU/ml. For the observation study of the time course of the pneumococcal invasive infection, the mice were monitored every 12 h for 12 days after the pneumococcal infection, as previously reported [28, 31]. If the mice were found to be severely sick (shivering, decreased motor activity), they were immediately euthanized and the blood was collected for confirmation of pneumococcus.

Nasal lavage sample collection

The mice were euthanized on the desired day and the nasal lavages were collected as previously described. To determine the bacterial density in the nasal cavity, the nasal lavages were serially diluted with sterile PBS, and were plated on sheep blood agar in triplicate overnight at 37°C, 5% CO_2. The colonies were counted for quantification of the bacteremia. The lower limit of detection (LOD) was 666 CFU/ml.

Blood sample collection

Blood from the euthanized mice was obtained by cardiac puncture with a 26 G needle, and collected in the tubes containing ethylene diamine tetra-acetic acid (EDTA) to avoid coagulation. The tubes were vortexed before the dilution and plating. After serial dilution with sterile PBS, the samples were plated on sheep blood agar in triplicate overnight at 37°C, 5% CO_2. The colonies were counted for the quantification of the bacteremia. The lower limit of detection (LOD) was 666 CFU/ml.

Flow cytometry

Neutrophil and macrophage cell counts were performed as previously described [28, 31]. The nasal lavages were pelleted at 1,500 rpm for 2 min, and resuspended in 200 μl PBS containing 1% bovine serum albumin (BSA). After FcR blocking with a 1:200 dilution of anti-CD16/32 (BioLegend, San Diego, CA, USA) for 15 min, cells were stained for 30 min at 4°C with 25 μl of 1:150 dilution of the following antibodies: anti-CD11b-V450 (BD Biosciences, San Jose, CA, USA), anti-F4/80-PE (BioLegend), anti-Ly6G-PerCP-Cy (BD Biosciences), and anti-CD45-APC-Cy7 (BD Biosciences) for 30 min on ice in the dark. Cells were washed with PBS with 1% BSA, then fixed with 4% PFA. FACS Verse (BD) was used for flow cytometry analysis. After excluding dead cells and debris by gating with forward and side scatter, neutrophils (polymorphonuclear cells; PMNs) were detected as $CD11b^+$, $Ly6G^+$, and $CD45^+$ components. Macrophages were detected as $F4/80^+$, $Ly6G^-$, and $CD45^+$ components (Supplementary Fig. 1). The absolute number of cells in each sample were counted.

Statistical analysis

Statistical analyses of the observation of the time course of pneumococcal invasive infection experiment were performed by using the Kaplan-Meier Log Rank test. Since the data were not confirmed whether they follow Gaussian distribution, Kruskal-Wallis test with Dunn's multiple comparison test was used to compare the bacterial load or the number of immune cells between more than two groups. The ratio of positive bacteremia was compared by Fisher's exact test. GraphPad Prism 8 (GraphPad Software, San Diego, CA, USA) was used for the analyses. The value $P<0.05$ served as the limit for the representation of significant differences.

Ethics statement

All studies were conducted according to the guidelines outlined by the National Science Foundation Animal Welfare Requirements and the Wakayama Medical University Animal Care and Use Committee. The study was approved by the Institutional Animal Care and Use Committee at Wakayama Medical University (permission number 28-42).

Results

A virulent strain serotype 6A and less virulent one, TIGR4 both established stable colonization among all mouse strains

To evaluate the role of nucleic sensing TLRs for pneumococcal carriage, mice were intranasally inoculated with 5×10^7 CFU of 6A strain without anesthesia. *S. pneumoniae* was successful in establishing nasal colonization in all mouse strains (Fig. 2A). Even when the mice were infected with influenza A virus (IAV) before or after pneumococcal inoculation, the density of nasal colonization was almost equal among all mouse strains (Figs. 2C and E). In this mouse model using a virulent pneumococcal strain, these TLRs did not affect the density of nasal colonization. Co-infection with influenza virus is known to increase the bacterial load in the nasal cavity, however, the significant difference was not observed between the infection models for each mouse strain (Figs. 2A, C and E). On the other hand, in the case of TIGR4 strain, TLR3 KO mice were more susceptible to having higher pneumococcal carriage in their nasal cavities (Supplementary Fig. 2A). Co-infection with IAV

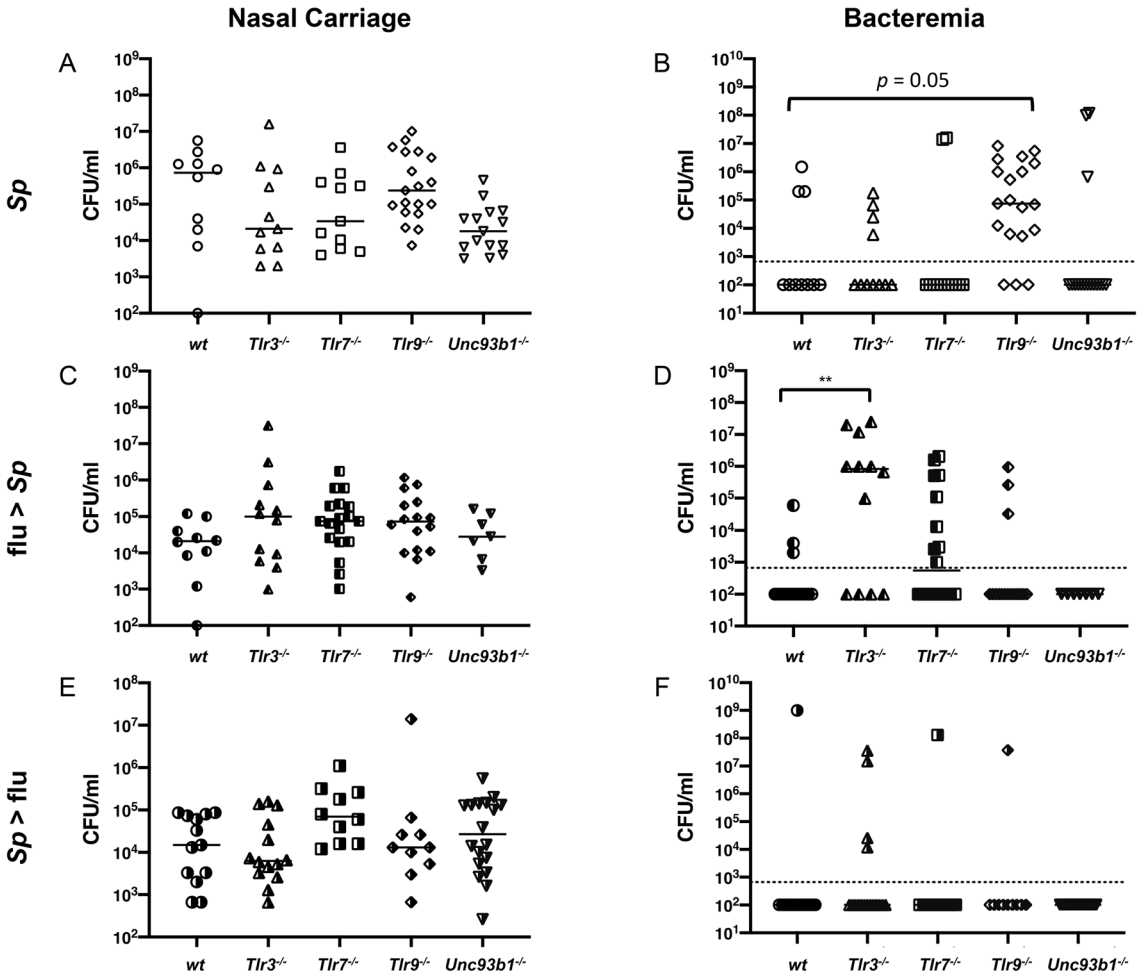

Fig. 2. Nasal colonization and bacteremia in each infection model of *S. pneumoniae* (*Sp*) 6A. A, B; the mono-infection model of *Sp*. The number of mice was 9 for *wt* (wildtype), 11 for *tlr3*$^{-/-}$ (TLR3 knockout), 11 for *tlr7*$^{-/-}$ (TLR7 knockout), 19 for *tlr9*$^{-/-}$ (TLR9 knockout), and 15 for *unc93b1*$^{-/-}$ (Unc93b1 knockout), respectively. C, D; the co-infection model (influenza first, then *Sp*). The number of mice was 10 for *wt*, 12 for *tlr3*$^{-/-}$, 18 for *tlr7*$^{-/-}$, 16 for *tlr9*$^{-/-}$, and 7 for *unc93b1*$^{-/-}$, respectively. E, F; the co-infection model (*Sp* first, then influenza). The number of mice was 13 for *wt*, 14 for *tlr3*$^{-/-}$, 10 for *tlr7*$^{-/-}$, 10 for *tlr9*$^{-/-}$, and 18 for *unc93b1*$^{-/-}$, respectively. A, B, C; nasal colonization and D, E, F; bacteremia. The pooled data of duplicated or triplicated experiment were displayed. All symbols represent individual data and the detection limit is 666 CFU/ml. **; $P<0.01$.

on day −2 and TIGR4 on day 0 did not cause any difference of pneumococcal carriage among mouse strains (Supplementary Fig. 2B).

Higher blood invasion was observed in TLR9 KO mice after pneumococcal mono-infection

Next, we investigated the early invasion of the bloodstream after nasal colonization with 6A strain. To exclude the possibility of bacteremia arising from pneumonia, lung homogenates from five wild-type mice were incubated and we confirmed there were no bacteria at the timing of blood sampling (data not shown). At 48 h after nasal inoculations of the bacteria, bacteremia was observed in a couple of mice of wildtype, TLR3 KO, TLR7 KO, and Unc93B1 KO strains, although those mice showed no symptoms of sepsis. The incidence rate of bacteremia was 30.0% (3 of 10) in wildtype, 36.4% (4 of 11) in TLR3 KO, 15.4% (2 out of 13) in TLR7 KO, and 18.8% (3 of 16) in Unc93b1 KO mice, respectively. Meanwhile, among TLR9 KO mice there was a significantly higher incidence of bacteremia (16 of 19, 84.2%), than in the other mouse strains (Fig. 2 and Table 1).

Co-infection with influenza increases the bacteremia rate in the TLR3 KO mice

As influenza virus co-infection is one of the most important factors in exacerbation of pneumococcal diseases, we evaluated pneumococcal bacteremia in mice co-infected with influenza. Two models of co-infection were established in different stage of influenza infection (Fig. 1). At first, co-infection with influenza virus was confirmed to enhance development of invasive pneumo-

Table 1. Summary of the incidence of bacteremia in different mouse strains

		Bacteremia (ratio)	*P*-value vs. wildtype by Fisher's exact test
Mono-infection (6A)	Wildtype	3/10 (30.0%)	-
	TLR3 KO	4/11 (36.4%)	0.76
	TLR7 KO	2/13 (15.4%)	0.40
	TLR9 KO	16/19 (84.2%)	0.0035
	Unc93b1 KO	3/16 (18.8%)	0.51
Co-infection (influenza first, then 6A)	Wildtype	3/15 (20.0%)	-
	TLR3 KO	8/12 (66.7%)	0.014
	TLR7 KO	9/18 (50.0%)	0.074
	TLR9 KO	3/16 (18.8%)	0.93
	Unc93b1 KO	0/7 (0.00%)	0.20
Co-infection (6A first, then influenza)	Wildtype	1/14 (7.14%)	-
	TLR3 KO	4/17 (23.5%)	0.22
	TLR7 KO	1/11 (9.09%)	0.86
	TLR9 KO	1/10 (10.0%)	0.80
	Unc93b1 KO	0/18 (0.00%)	0.25

coccal infection among wildtype mice in the current model. The incidence of invasive pneumococcal infection was higher in the co-infection models than the mono-infection model. In particular, significant difference was observed in survival curve between the mono-infected model and the co-infection model of prior flu infection ($P<0.05$ by Log-rank test) (Figs. 4A–C). When the mice were given influenza before the pneumococcal infection, the pneumococcus invaded the bloodstream more frequently among TLR3 KO mice (8/12, 66.7%) and TLR7 KO mice (9/18, 50%) than in wildtype mice (3/15, 20%). Particularly, TLR3 KO mice had a statistically higher density of bacteremia and higher ratio of developing bacteremia than the wildtype (Fig. 2D and Table 1). In contrast to pneumococcal mono-infection, the ratio of bacteremia was low in TLR9 KO mice (3/16, 18.8%) a similar level to that of wildtype mice. Furthermore, Unc93b1 KO mice did not develop bacteremia (0/7, 0%). In the case of influenza and TIGR4 co-infection, the mice did not develop bacteremia (data not shown).

On the other hand, the timing of the co-infection greatly affected the ratio of bacteremia development. When influenza was infected after the 6A inoculum, the bacteremia rate was low among all mouse strains: wildtype (1/14, 7.14%), TLR3 KO (4/17, 23.5%), TLR7 KO (1/11, 9.09%), TLR9 KO (1/10, 10.0%) and Unc93b1 KO mice (0/18, 0%) (Fig. 2F and Table 1).

Impact of nucleic sensing TLRs on the local influx of immune cells

In the mono-infection model, the number of neutrophils in the nasal lavage did not differ between mouse strains (Fig. 3A), while the influx of macrophages was significantly increased among TLR7 KO and TLR9 KO mouse strains (wildtype vs TLR7 KO; $P<0.01$, wildtype vs TLR9 KO; $P<0.05$) (Fig. 3B). In the state of pre-infection with influenza virus, the migration of neutrophils in the nasal cavity was significantly inhibited in the mice lacking TLR3 and Unc93b1 (wildtype vs TLR3 KO; $P<0.01$, wildtype vs Unc93b1 KO; $P<0.01$) (Fig. 3C). A similar change of neutrophils was observed for macrophage that significantly decreased in TLR3 KO and Unc93b1 KO strains (wildtype vs TLR3 KO; $P<0.05$, wildtype vs Unc93b1 KO; $P<0.05$) (Fig. 3D). Even when the influenza infection followed the pneumococcal inoculum, the migration of neutrophils was significantly suppressed in TLR3 KO and Unc93b1 KO mouse strains compared with that in wildtype mice (wildtype vs TLR3 KO; $P<0.05$, wildtype vs Unc93b1 KO; $P<0.0001$) (Fig. 3E). The difference of the number of macrophages between the wildtype, TLR3 KO and Unc93b1 KO mice disappeared when the order of influenza and pneumococcal infection changed (Fig. 3F).

Suppression of nucleic sensing TLRs worsened the prognosis of pneumococcal invasive infection in the mono-infection model

The survival of the mice was measured every 12 h and the severely sick mice showing shivering, messy hair and loss of activity were immediately euthanized and bacteremia was confirmed by cardiac puncture. In the pneumococcal mono-infection model, all knockout mouse strains showed significantly poorer survival than that of wildtype (13/14, 92.9%); TLR3 KO (10/18, 55.6%, $P<0.05$), TLR7 KO (5/12, 41.7%, $P<0.05$), TLR9 KO (6 out of 12, 50.0%, $P<0.0001$) and Unc93b1 KO mice (4 out of 10, 40.0%, $P<0.01$) (Fig. 4A). The result in TLR9 KO mice is supported by the high prevalence of bacteremia at 48 h after nasal inoculum. Although the

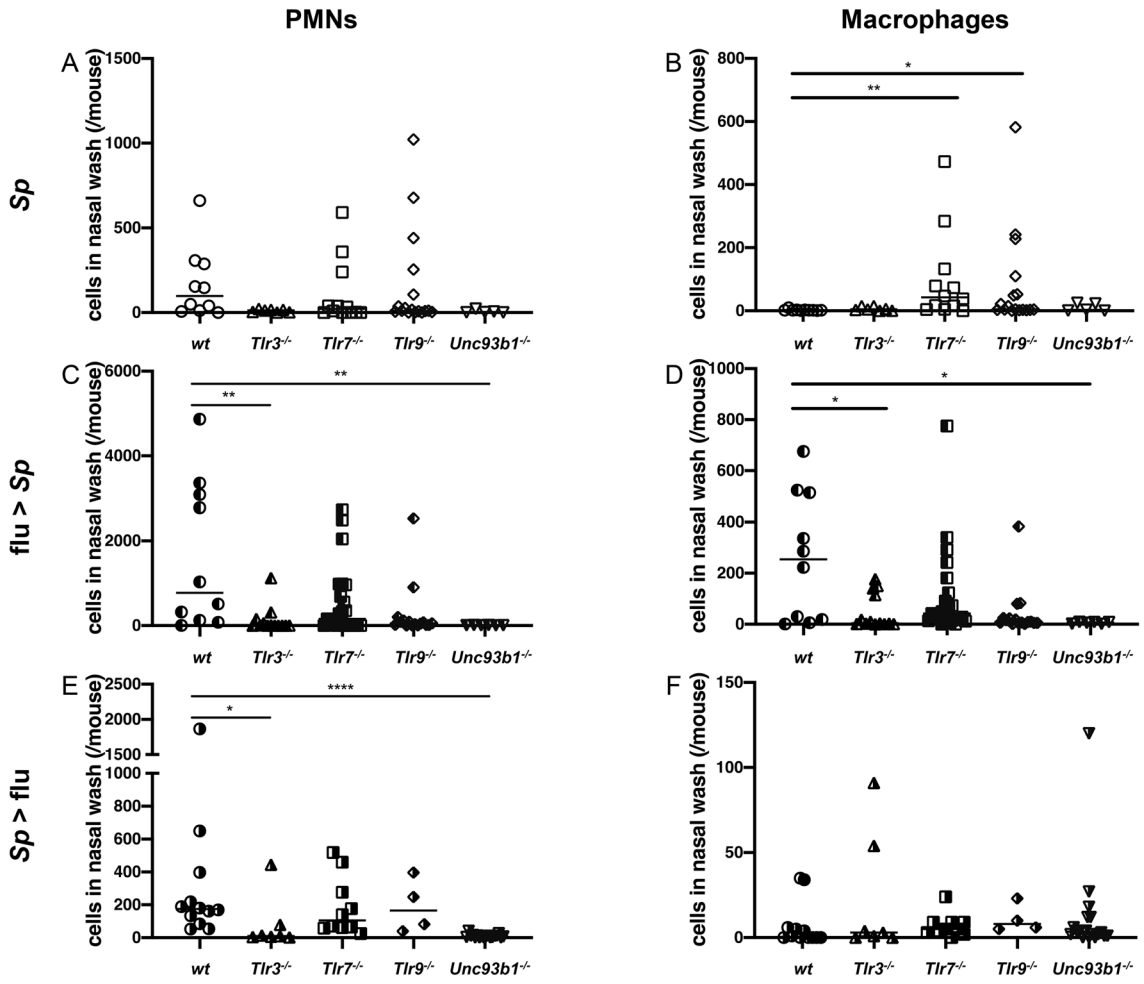

Fig. 3. The local influx of PMNs and macrophages in each infection model of *S. pneumoniae* (*Sp*) 6A. A, B; the mono-infection model of *Sp*. The number of mice was 10 for *wt* (wildtype), 7 for *tlr3*$^{-/-}$ (TLR3 knockout), 12 for *tlr7*$^{-/-}$ (TLR7 knockout), 17 for *tlr9*$^{-/-}$ (TLR9 knockout), and 5 for *unc93b1*$^{-/-}$ (Unc93b1 knockout), respectively. C, D; the co-infection model (influenza first, then *Sp*). The number of mice was 10 for *wt*, 13 for *tlr3*$^{-/-}$, 23 for *tlr7*$^{-/-}$, 16 for *tlr9*$^{-/-}$, and 6 for *unc93b1*$^{-/-}$, respectively. E, F; the co-infection model (*Sp* first, then influenza). The number of mice was 12 for *wt*, 7 for *tlr3*$^{-/-}$, 10 for *tlr7*$^{-/-}$, 4 for *tlr9*$^{-/-}$, and 18 for *unc93b1*$^{-/-}$, respectively. A, B, C; Polymorphonuclear Cells (PMNs) in the nasal lavage and D, E, F; macrophages in the nasal lavage. The pooled data of duplicated or triplicated experiment were displayed. Every symbol represents individual data. *; $P<0.05$, **; $P<0.01$, and ****; $P<0.0001$.

other TLR KO and Unc93b1 KO mice showed less occurrence of bacteremia at 48 h after pneumococcal infection, the course of invasive infection was similar to TLR9 KO mouse group, suggesting that both TLR3 and TLR7 signaling might be important for protecting the development of lethal infection after pneumococcal invasion into the bloodstream.

Effect of influenza co-infection on the course of pneumococcal invasive infection

When the mice were infected with influenza before pneumococcal infection, the survival rate was decreased in all mouse strains; wildtype (6/12, 50%), TLR3 KO (3/8, 37.5%), TLR7 KO (5/16, 31.3%), TLR9 KO (5/15, 33.3%) and Unc93b1 KO mice (4/21, 19.0%) (Fig. 4B). In particular, the wildtype mice precedingly infected with influenza before *S. pneumoniae* inoculum showed significantly poorer survival than those infected *S. pneumoniae* only ($P<0.05$) (Figs. 4A and B). However, when the mice were pre-infected with *S. pneumoniae* and later with influenza, the time course of the lethal infection was similar to that with pneumococcal mono-infection among all mouse strains, with the exception of TLR3 KO strain. A lack of TLR3 signaling showed the most susceptibility to pneumococcal invasive infection with this co-infection model (2/12, 16.7%) compared with the other strains; wildtype mice (5/7, 71.4%, $P<0.05$), TLR7 KO (4/8, 50.0%, not significant), TLR9 KO mice (7/16, 43.8%, $P<0.05$) and Unc93b1 KO mice (4/7, 57.4%, $P=0.05$) (Fig. 4C).

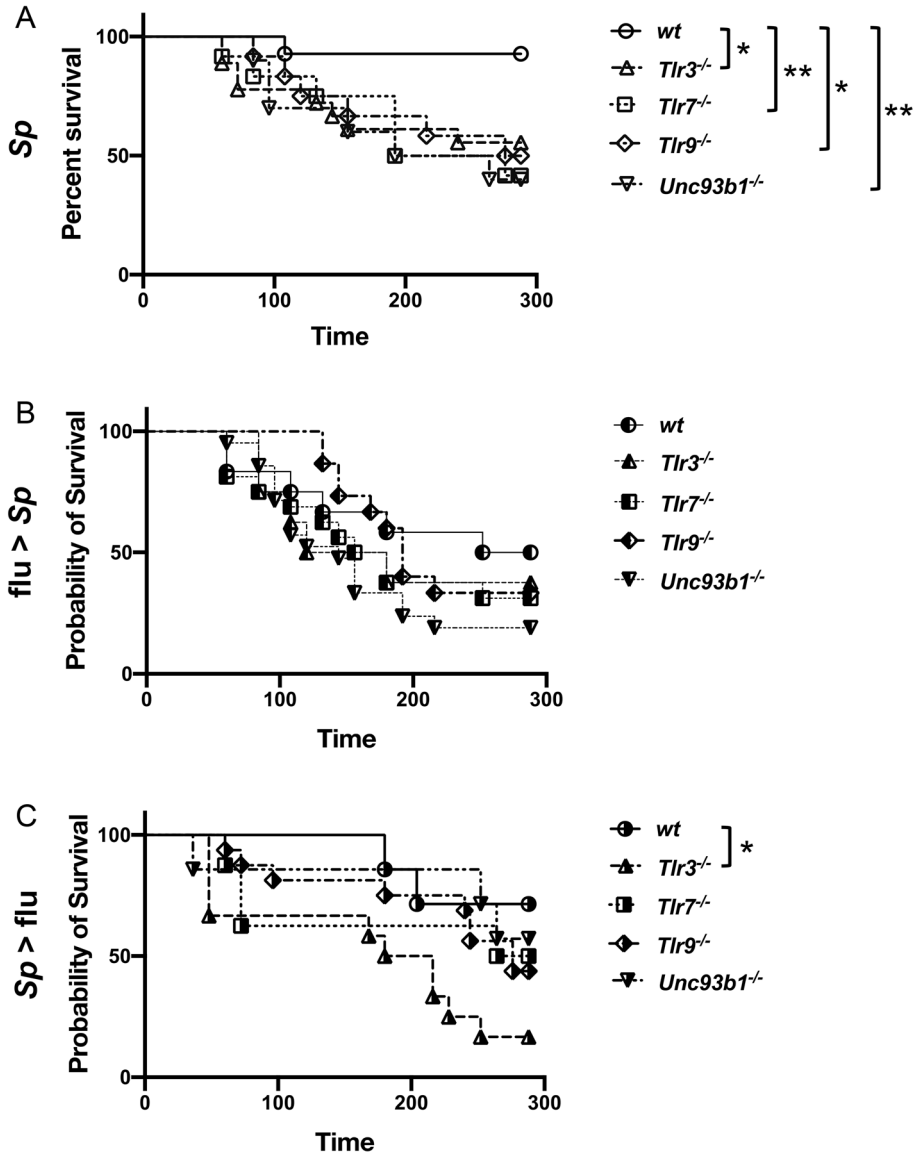

Fig. 4. The time course of development of invasive infection of *S. pneumoniae* (*Sp*) 6A. After intranasal administration of *Sp*, the mice were monitored every 12 h until day 12 (endpoint). A; the mono-infection model of *Sp*. The number of mice was 14 for *wt* (wildtype), 18 for *tlr3*$^{-/-}$ (TLR3 knockout), 12 for *tlr7*$^{-/-}$ (TLR7 knockout), 12 for *tlr9*$^{-/-}$ (TLR9 knockout), and 10 for *unc93b1*$^{-/-}$ (Unc93b1 knockout), respectively. B; the co-infection model (influenza first, then *Sp*). The number of mice was 12 for *wt*, 8 for *tlr3*$^{-/-}$, 16 for *tlr7*$^{-/-}$, 15 for *tlr9*$^{-/-}$, and 21 for *unc93b1*$^{-/-}$, respectively. and C; the co-infection model (*Sp* first, then influenza). The number of mice was 7 for *wt*, 12 for *tlr3*$^{-/-}$, 8 for *tlr7*$^{-/-}$, 16 for *tlr9*$^{-/-}$, and 7 for *unc93b1*$^{-/-}$, respectively. The pooled data of duplicated or triplicated experiment were displayed. *; $P<0.05$, **; $P<0.01$.

Discussion

Nasal colonization is a significant phase of the onset and the development of pneumococcal diseases. When the bacteria in the nasal cavity directly access the bloodstream, they must overcome stringent mucosal barriers. Pneumococcus colonized in hosts receive a strong selective pressure while developing bacteremia, the so-called 'bottleneck effect' [28]. The killing of bacteria by immune cells and the epithelial barrier at the nasal cavity are the first line of defense and the ability of bacteria to translocate from the extracellular matrix through the endothelium is affected by the presence of the innate immune system members, such as TLRs [32–34]. We focused on neutrophils and macrophages those have been reported to be critical for clearance of pneumococcal colonization from the nasal cavity [35, 36]. Our results that the mice inhibited TLR3 signaling (TLR3 KO mouse and Unc93b1 KO mouse) showed impaired influx of neutrophils and macrophages by co-infection with flu, a

strong agonist of TLR3, are consistent, partially reflecting the prognosis of pneumococcal systemic infection. Recently, the importance of natural killer cells as a defense mechanism against both bacterial and viral infections has been reported. In particular, it has been pointed out that TLR7 activates natural killer cells during influenza virus infection, which might impact on the results of this study [37]. To model pneumococcal occult bacteremia without pneumonia usually occurring in children, we introduced a virulent strain serotype 6A [28]. Furthermore, to avoid a direct influx of bacterial suspension to the lung, we inoculated the bacteria in the nose without anesthesia [28, 31].

All mice had similar nasal colonization in the current three infection models. After establishing stable nasal colonization, the pneumococcus invades into the basal layer of tissue where the bacteria can access the bloodstream [28]. Our previous work demonstrated that the pneumococcus could reach under the epithelial cell layer by passing through intercellular space [38]. When the bacteria enter the systemic circulation, most cells of the pneumococcus are entrapped and killed in the spleen. On the other hand, very few pneumococcal cells survive in the spleen invade into the bloodstream again and develop lethal infection "bacteremia/sepsis" [39, 40]. These findings suggest the pneumococcus has to conquer at least two tight bottlenecks; nasal epithelium and spleen, for developing lethal infection. In the pneumococcal mono-infection model, only TLR9 KO mice showed a high prevalence of bacteremia, which suggests that TLR9 signaling is one of the key factors in regulation of the bottleneck between the nasal cavity and blood. Data on survival of mono-infection were consistent for TLR9 KO mice, which had the lowest rate of survival. This finding is important because only one previous study observed the role of TLR9 in triggering the activation of resident macrophages and early bacterial clearance in pneumococcal infections [23]. On the other hand, TLR3 KO, TLR7 KO, and Unc93b1 KO mice also showed poor prognosis compared with wildtype mice. Each of these nucleic acid sensing receptors is thus suggested to have a critical role in the prevention of developing sepsis from bacteremia.

A critical part of our experiment is the determination of the differences in nasal colonization and survival in co-infection with influenza virus compared with pneumococcal mono-infection. A pneumococcal infection is a major reason for high mortality during outbreaks of influenza virus, [41, 42] and a very influential factor in the establishment of colonization of pneumococcus in the upper respiratory tract due to the increased inflammation [28, 30]. Contrary to the mono-infection model, TLR9 KO mice did not develop bacteremia in the co-infection state with the influenza virus. The absence of bacteremia in this model suggests that the other TLRs have been activated by the influenza infection, which affected the inflammatory responses after *S. pneumoniae* inoculum, resulting in the inhibition of bacteremia.

In this co-infection model, TLR3 KO mice had the highest progress of bacteria in the blood. TLR3 is known to recognize the double-stranded RNA genetic material of viruses [17]. This high bacteremia development may be due to the deletion of TLR3, which has enabled the influenza virus to be unrecognized by the signaling pathways, easily replicating and increasing inflammation in the cavity, leading to disruption of the mucosal barrier. Furthermore, two previous studies have shown that the endosomal TLR3 recognizes pneumococcal nucleic acid during infection, and it may induce IL-12p70 secretion as an anti-pneumococcal response [20, 21]. Activation of TLR3 signaling by pneumococcal nucleic acid recognition may, however, be limited in the current model. Our findings support the idea that TLR3 plays a key role in preventing bacteremia in post-influenza pneumococcal disease. Once the pneumococci invaded the bloodstream, the onset of sepsis was similar to all of the four knockout groups, while the wildtype mice showed a better predisposition to survival. A study focused on a gram-positive *Staphylococcus aureus* conveyed the importance of neutrophils in controlling the nasal load and preventing bacterial pneumonia, as they block the dissemination of bacteria from the upper to the lower airways [43]. According to our results, TLR3 KO mice had the lowest level of neutrophils in both 6A mono-infection and co-infection model. This neutropenia may explain the uncontrolled spread of pneumococci during the state of co-infection. However, in co-infection, TLR9 KO mice in the co-infection model had a higher number of neutrophils in the nasal load than in TLR3 KO strain (not significant), making it a good candidate for explaining the low development of bacteremia in this model.

Nucleic sensing TLRs were shown in a recent study to potentially play a role in the recognition of the pneumococcus, and the importance of TLR7 and TLR9 in pneumococcal infections was shown. The mice with single deletions (TLR7, TLR9, or TLR13) were affected mostly by the spread of pneumococcus in the lungs and by the progress of encephalitis [21]. An intriguing finding of that study was the ability of these TLRs to act instead of each other and the absence of TLRs can indemnify the loss of other endosomal receptors. This may be one explanation for our result of the time course of invasive infection. They also demonstrated the dominant role of those TLRs in developing bacteremia/sepsis, but

their bacteremia model was via pneumococcal pneumonia. The major differences in our study are that the strain we mainly used, serotype 6A, is more virulent than TIGR4, which was used in their study, and that the procedure of intranasal inoculation was performed without anesthesia in order to avoid the direct invasion of the bacteria to the lower respiratory tract, as we previously reported in a model of pneumococcal pneumonia with TIGR4 strain by intranasal inoculation under anesthesia. Over-stimulation of the TLR9 by the agonist CpG-ODN was shown in a recent study to increase the bacteria clearance and the survival in the murine model. Our study helps to explain the previous study because TLR9 seems to be a major factor in the development of invasive pneumococcal diseases [44].

In this study, TLR3 and TLR9 showed the great impact on mouse survival. The main signaling system of TLRs including TLR7 and TLR9 is MyD88 dependent. MyD88 associates with IRAK4 (IL-1 receptor-associated kinase 4) that induces phosphorylation of IRAK1. As a result of the activation of NFκB, inflammatory cytokines such as TNF-α and IL-12 are produced, and inflammatory cells necessary for elimination of pneumococci migrate into the nasal cavity. In the mono-infection model, TLR9 was thought to recognize pneumococcal DNA and induce anti-pneumococcal immune responses. On the other hand, TLR3, which recognizes viral double strand RNA, activates TRIF mediated signaling system. Unlike MyD88 mediated signaling, IKKi/IKKe and TBK1 activate the transcription factor IRAF3 and induce type I interferon. In the co-infection model, especially when the pneumococci are administered to mice in advance and then infected with influenza virus, TLR3 KO mice showed the worst survival. A possible reason is when flu infected in the nasal cavity where the pneumococci already established their colonization, barriers of nasal epithelium were significantly disrupted by flu-induced inflammation in the absence of TLR3 dependent immune responses, which would help the pneumococci invade into deeper tissue. Further study should be addressed to elucidate detailed activation mechanism of the signaling pathway in the infection model by multiple pathogens.

The effects seen in single TLR KO mice were not necessarily invaginated in Unc93b1 KO mice. There are two possible reasons to explain the discrepancy. First, TLRs share common signaling pathways such as MyD88 and TRIF. For example, pneumococcal teichoic acid and pneumolysin can stimulate TLR2 and TLR4 respectively, that results activation of both MyD88 and TRIF mediated pathways. Blocking one TLR signaling may not have resulted in the expected response due to positive/negative feedback systems of other TLR signaling pathways. Second, in order to establish an animal model in which all signaling pathways of TLR3, TLR7, and TLR9 are blocked, we introduced a mouse strain knocked out of Unc93b1, a protein required for activating these endosome-located TLRs. To construct a rigorous model, it would be ideal to generate a mouse strain with triple TLRs knock out.

In this report, we demonstrated that nucleic sensing TLRs play a dominant role in the acquisition of pneumococcal invasion in adult mouse models. However, the findings of this study have to be seen in the light of a limitation caused by the lack of data of a model of a mouse where all the three TLR deletions are implemented; this limitation should be addressed in future research. Further studies are required to test the mechanism responsible for explaining why the TLR9 is effective in the control of the invasion and the mechanism other TLRs compensate for the lack of each other, leading to similar survival in the murine model. On the other hand, a study based on the effect of Gram-negative bacteria or a less invasive Gram-positive *S. pneumoniae* serotype in the same murine model is necessary for understanding the pneumococcal factor responsible for these differences. The bacteremia level was higher in all the mice when they were pre-infected with influenza compared with the case when they were pre-infected with *S. pneumoniae* and later influenza. Other studies have shown that preceding colonization with *S. pneumoniae* actually reduces influenza infection [45–47].

In conclusion, the current findings related to the nucleic acid-sensing, TLR9, and its phenotypic differences are promising, and future studies will aim to gain better understanding of the mechanism.

Funding

This work was supported by JSPS KAKENHI Grant Number 20K08825 and Young Researcher Support Grant of Wakayama Medical University to MK.

Conflicts of Interest

The authors declare no conflicts of interest associated with this study.

Acknowledgments

We thank Professor Kensuke Miyake at the University of Tokyo, Professor Tsuneyasu Kaisho at Wakayama Medical University, and Professor Shizuo Akira at Osaka University for providing knockout mouse strains. We also thank Professor Jeffery N. Weiser at New York

University for providing pneumococcal and influenza strains. We acknowledge editing and proofreading by Benjamin Phillis from the Clinical Study Support Center at Wakayama Medical University.

References

1. Desamero MJM, Chung SH, Kakuta S. Insights on the functional role of beta-glucans in fungal immunity using receptor-deficient mouse models. Int J Mol Sci. 2021; 22: 4778. [Medline] [CrossRef]
2. Tang C, Kakuta S, Shimizu K, Kadoki M, Kamiya T, Shimazu T, et al. Suppression of IL-17F, but not of IL-17A, provides protection against colitis by inducing T_{reg} cells through modification of the intestinal microbiota. Nat Immunol. 2018; 19: 755–765. [Medline] [CrossRef]
3. Kaur R, Pham M, Pichichero M. Serum antibody levels to pneumococcal polysaccharides 22F, 33F, 19A and 6A that correlate with protection from colonization and acute otitis media in children. Vaccine. 2021; 39: 3900–3906. [Medline] [CrossRef]
4. Huang CC, Chang TH, Lee CY, Wu PW, Chen CL, Lee TJ, et al. Tissue microbiota in nasopharyngeal adenoid and its association with pneumococcal carriage. Microb Pathog. 2021; 157: 104999. [Medline] [CrossRef]
5. Bonko MDA, Lompo P, Tahita MC, Kiemde F, Karama I, Somé AM, et al. Antibiotic susceptibility of *Staphylococcus aureus* and *Streptococcus pneumoniae* isolates from the nasopharynx of febrile children under 5 years in Nanoro, Burkina Faso. Antibiotics (Basel). 2021; 10: 444. [Medline] [CrossRef]
6. Ali MQ, Kohler TP, Burchhardt G, Wüst A, Henck N, Bolsmann R, et al. Extracellular pneumococcal serine proteases affect nasopharyngeal colonization. Front Cell Infect Microbiol. 2021; 10: 613467. [Medline] [CrossRef]
7. Zangari T, Ortigoza MB, Lokken-Toyli KL, Weiser JN. Type I interferon signaling is a common factor driving *Streptococcus pneumoniae* and influenza A virus shedding and transmission. mBio. 2021; 12: e03589-20. [Medline] [CrossRef]
8. Murakami D, Kono M, Nanushaj D, Kaneko F, Zangari T, Muragaki Y, et al. Exposure to cigarette smoke enhances pneumococcal transmission among littermates in an infant mouse model. Front Cell Infect Microbiol. 2021; 11: 651495. [Medline] [CrossRef]
9. Zafar MA, Kono M, Wang Y, Zangari T, Weiser JN. Infant mouse model for the study of shedding and transmission during *Streptococcus pneumoniae* mono-infection. Infect Immun. 2016; 84: 2714–2722. [Medline] [CrossRef]
10. Loughran AJ, Orihuela CJ, Tuomanen EI. *Streptococcus pneumoniae*: Invasion and Inflammation. Microbiol Spectr. 2019; 7: [CrossRef]. [Medline]
11. Liu G, Zhang H, Zhao C, Zhang H. Evolutionary history of the Toll-like receptor gene family across vertebrates. Genome Biol Evol. 2020; 12: 3615–3634. [Medline] [CrossRef]
12. Too LK, Yau B, Baxter AG, McGregor IS, Hunt NH. Double deficiency of toll-like receptors 2 and 4 alters long-term neurological sequelae in mice cured of pneumococcal meningitis. Sci Rep. 2019; 9: 16189. [Medline] [CrossRef]
13. Chen X, Meng X, Foley NM, Shi X, Liu M, Chai Y, et al. Activation of the TLR2-mediated downstream signaling pathways NF-κB and MAPK is responsible for B7-H3-augmented inflammatory response during *S. pneumoniae* infection. J Neuroimmunol. 2017; 310: 82–90. [Medline] [CrossRef]
14. Sun X, Wang J, Zhou J, Wang H, Wang X, Wu J, et al. Subcutaneous immunization with *Streptococcus pneumoniae* GAPDH confers effective protection in mice via TLR2 and TLR4. Mol Immunol. 2017; 83: 1–12. [Medline] [CrossRef]
15. Shu Z, Yuan J, Wang H, Zhang J, Li S, Zhang H, et al. *Streptococcus pneumoniae* PepO promotes host anti-infection defense via autophagy in a Toll-like receptor 2/4 dependent manner. Virulence. 2020; 11: 270–282. [Medline] [CrossRef]
16. Akira S, Takeda K. Toll-like receptor signalling. Nat Rev Immunol. 2004; 4: 499–511. [Medline] [CrossRef]
17. Alexopoulou L, Holt AC, Medzhitov R, Flavell RA. Recognition of double-stranded RNA and activation of NF-kappaB by Toll-like receptor 3. Nature. 2001; 413: 732–738. [Medline] [CrossRef]
18. Hemmi H, Kaisho T, Takeuchi O, Sato S, Sanjo H, Hoshino K, et al. Small anti-viral compounds activate immune cells via the TLR7 MyD88-dependent signaling pathway. Nat Immunol. 2002; 3: 196–200. [Medline] [CrossRef]
19. Ohto U, Shibata T, Tanji H, Ishida H, Krayukhina E, Uchiyama S, et al. Structural basis of CpG and inhibitory DNA recognition by Toll-like receptor 9. Nature. 2015; 520: 702–705. [Medline] [CrossRef]
20. Spelmink L, Sender V, Hentrich K, Kuri T, Plant L, Henriques-Normark B. Toll-like receptor 3/TRIF-dependent IL-12p70 secretion mediated by *Streptococcus pneumoniae* RNA and its priming by influenza A virus coinfection in human dendritic cells. MBio. 2016; 7: e00168-16. [Medline] [CrossRef]
21. Famà A, Midiri A, Mancuso G, Biondo C, Lentini G, Galbo R, et al. Nucleic acid-sensing Toll-like receptors play a dominant role in innate immune recognition of pneumococci. MBio. 2020; 11: e00415-20. [Medline] [CrossRef]
22. Stegemann S, Dahlberg S, Kröger A, Gereke M, Bruder D, Henriques-Normark B, et al. Increased susceptibility for superinfection with *Streptococcus pneumoniae* during influenza virus infection is not caused by TLR7-mediated lymphopenia. PLoS One. 2009; 4: e4840. [Medline] [CrossRef]
23. Albiger B, Dahlberg S, Sandgren A, Wartha F, Beiter K, Katsuragi H, et al. Toll-like receptor 9 acts at an early stage in host defence against pneumococcal infection. Cell Microbiol. 2007; 9: 633–644. [Medline] [CrossRef]
24. Lee KS, Scanga CA, Bachelder EM, Chen Q, Snapper CM. TLR2 synergizes with both TLR4 and TLR9 for induction of the MyD88-dependent splenic cytokine and chemokine response to *Streptococcus pneumoniae*. Cell Immunol. 2007; 245: 103–110. [Medline] [CrossRef]
25. Honda K, Sakaguchi S, Nakajima C, Watanabe A, Yanai H, Matsumoto M, et al. Selective contribution of IFN-alpha/beta signaling to the maturation of dendritic cells induced by double-stranded RNA or viral infection. Proc Natl Acad Sci USA. 2003; 100: 10872–10877. [Medline] [CrossRef]
26. Hemmi H, Takeuchi O, Kawai T, Kaisho T, Sato S, Sanjo H, et al. A Toll-like receptor recognizes bacterial DNA. Nature. 2000; 408: 740–745. [Medline] [CrossRef]
27. Fukui R, Saitoh S, Kanno A, Onji M, Shibata T, Ito A, et al. Unc93B1 restricts systemic lethal inflammation by orchestrating Toll-like receptor 7 and 9 trafficking. Immunity. 2011; 35: 69–81. [Medline] [CrossRef]
28. Kono M, Zafar MA, Zuniga M, Roche AM, Hamaguchi S, Weiser JN. Single Cell Bottlenecks in the Pathogenesis of *Streptococcus pneumoniae*. PLoS Pathog. 2016; 12: e1005887. [Medline] [CrossRef]
29. Liang S, Mozdzanowska K, Palladino G, Gerhard W. Heterosubtypic immunity to influenza type A virus in mice. Effector mechanisms and their longevity. J Immunol. 1994; 152: 1653–1661. [Medline] [CrossRef]
30. Richard AL, Siegel SJ, Erikson J, Weiser JN. TLR2 signaling decreases transmission of *Streptococcus pneumoniae* by limiting bacterial shedding in an infant mouse Influenza A co-infection model. PLoS Pathog. 2014; 10: e1004339. [Medline] [CrossRef]
31. Kono M, Nanushaj D, Sakatani H, Murakami D, Hijiya M, Kinoshita T, et al. The roles of transient receptor potential vanilloid 1 and 4 in pneumococcal nasal colonization and subsequent development of invasive disease. Front Immunol. 2021; 12: 732029. [Medline] [CrossRef]

32. Martín-Hernández D, Caso JR, Bris ÁG, Maus SR, Madrigal JL, García-Bueno B, et al. Bacterial translocation affects intracellular neuroinflammatory pathways in a depression-like model in rats. Neuropharmacology. 2016; 103: 122–133. [Medline] [CrossRef]
33. Hiemstra IH, Bouma G, Geerts D, Kraal G, den Haan JM. Nod2 improves barrier function of intestinal epithelial cells via enhancement of TLR responses. Mol Immunol. 2012; 52: 264–272. [Medline] [CrossRef]
34. Clarke TB, Francella N, Huegel A, Weiser JN. Invasive bacterial pathogens exploit TLR-mediated downregulation of tight junction components to facilitate translocation across the epithelium. Cell Host Microbe. 2011; 9: 404–414. [Medline] [CrossRef]
35. Siegel SJ, Tamashiro E, Weiser JN. Clearance of pneumococcal colonization in infants is delayed through altered macrophage trafficking. PLoS Pathog. 2015; 11: e1005004. [Medline] [CrossRef]
36. Kaneko F, Kono M, Sunose H, Hotomi M. Neutrophil infiltration in co-housed littermates plays a key role in nasal transmission of *Streptococcus pneumoniae* in an infant mouse model. Folia Microbiol (Praha). 2022; 67: 45–54. [Medline] [CrossRef]
37. Stegemann-Koniszewski S, Behrens S, Boehme JD, Hochnadel I, Riese P, Guzmán CA, et al. Respiratory influenza A virus infection triggers local and systemic natural killer cell activation via Toll-like receptor 7. Front Immunol. 2018; 9: 245. [Medline] [CrossRef]
38. Takeda S, Kono M, Sugita G, Arai J, Briles DE, Hotomi M. Pneumococcal capsular phase shift is associated with invasion into cell-to-cell junctions and is inhibited by macrolides. Microb Pathog. 2021; 153: 104787. [Medline] [CrossRef]
39. Gerlini A, Colomba L, Furi L, Braccini T, Manso AS, Pammolli A, et al. The role of host and microbial factors in the pathogenesis of pneumococcal bacteraemia arising from a single bacterial cell bottleneck. PLoS Pathog. 2014; 10: e1004026. [Medline] [CrossRef]
40. Ercoli G, Fernandes VE, Chung WY, Wanford JJ, Thomson S, Bayliss CD, et al. Intracellular replication of *Streptococcus pneumoniae* inside splenic macrophages serves as a reservoir for septicaemia. Nat Microbiol. 2018; 3: 600–610. [Medline] [CrossRef]
41. Shirey KA, Perkins DJ, Lai W, Zhang W, Fernando LR, Gusovsky F, et al. Influenza "Trains" the host for enhanced susceptibility to secondary bacterial infection. MBio. 2019; 10: e0081-19. [Medline] [CrossRef]
42. Morris DE, Cleary DW, Clarke SC. Secondary bacterial infections associated with influenza pandemics. Front Microbiol. 2017; 8: 1041. [Medline] [CrossRef]
43. Rigby KM, DeLeo FR. Neutrophils in innate host defense against Staphylococcus aureus infections. Semin Immunopathol. 2012; 34: 237–259. [Medline] [CrossRef]
44. Ribes S, Zacke L, Nessler S, Saiepour N, Avendaño-Guzmán E, Ballüer M, et al. Oligodeoxynucleotides containing unmethylated cytosine-guanine motifs are effective immunostimulants against pneumococcal meningitis in the immunocompetent and neutropenic host. J Neuroinflammation. 2021; 18: 39. [Medline] [CrossRef]
45. McCullers JA, Rehg JE. Lethal synergism between influenza virus and *Streptococcus pneumoniae*: characterization of a mouse model and the role of platelet-activating factor receptor. J Infect Dis. 2002; 186: 341–350. [Medline] [CrossRef]
46. Diavatopoulos DA, Short KR, Price JT, Wilksch JJ, Brown LE, Briles DE, et al. Influenza A virus facilitates *Streptococcus pneumoniae* transmission and disease. FASEB J. 2010; 24: 1789–1798. [Medline] [CrossRef]
47. Shinya K, Okamura T, Sueta S, Kasai N, Tanaka M, Ginting TE, et al. Toll-like receptor pre-stimulation protects mice against lethal infection with highly pathogenic influenza viruses. Virol J. 2011; 8: 97. [Medline] [CrossRef]